SEMI-ANALYTICAL MODELLING OF HELICOPTER MAIN ROTOR NOISE[†]

G. REBOUL[‡]
ONERA (DSNA/ACOU)
29 av. de la Division Leclerc
FR-92320 Châtillon

A. TAGHIZAD
ONERA (DCSD/PSEV)
Base Aérienne 701
FR-13661 Salon de Provence

Abstract

A simplified semi-analytical model aiming to predict the noise emitted by the main rotor of a helicopter with emphasis on the loading noise due to blade-vortex interaction is presented in this paper. The goal of this model is to be used together with the flight mechanics code EUROPA and should consequently have the same level of modelling. Each step of development is detailed and compared with the state of art ONERA comprehensive code HMMAP. It arises that main discrepancies are due to the wake geometry prediction, when a prescribed wake is used instead of a free wake code. On the contrary, the use of analytical response function provides rather good results by comparison with the singularity method implemented in HMMAP. This paper also demonstrates that a good acoustic prediction can not be achieved without a good rotor thrust evaluation. Nevertheless, it is found that satisfactory results, that could be used for preliminary studies, can be obtained with such a fast and simplified model.

NOTATION

B	number of blade
b	semi-airfoil chord, m
c	airfoil chord, m
Cl_α	lift curve slope, rad^{-1}
C_n	normal force coefficient
c_0	speed of sound, m/s
h	blade vortex distance, m
M	blade element relative Mach number
R	rotor radius, m
r	blade element radial position, m
r_c	vortex viscous core radius, m
S_g	aerodynamic blade function transfer
T	thrust, N
U_p	blade element normal velocity, m/s
U_t	blade element tangential velocity, m/s
V_0	wind speed, m/s
w	vortex induced upwash velocity fluctuation, m/s
α	aerodynamic angle of attack, $^\circ$
α_s	rotor shaft angle of attack, $^\circ$
β	flapping angle, $^\circ$
χ	blade-vortex angle, $^\circ$
Γ	vortex intensity, m^2/s
Ω	rotational speed, rad/s
φ	azimuth, $^\circ$
θ	blade pitch angle, $^\circ$
θ_v	blade pitch angle induced by twist, $^\circ$
ν	rotor induced velocity, m/s
BVI	Blade Vortex Interaction
BPF	Blade Passing Frequency
FW-H	Ffowcs Williams – Hawkings
HART	Higher harmonic control Aeroacoustic Rotor Test
SPL	Sound Pressure Level

INTRODUCTION

Since the noise impact reduction is now a strong requirement for future rotorcraft (both civil and military), it is necessary to take into account this parameter at early stage of each helicopter development. Preliminary studies involve a great number of design parameters but also of flight conditions. Consequently, the tools used for noise reduction studies need to be fast but accurate enough to discriminate noisy design with a reduce number of input data. The need of such a tool have been identified in two current projects where ONERA is involved.

[†] Presented at the 38th European Rotorcraft Forum, Amsterdam, Netherlands, September 4-7, 2012

[‡] Corresponding author: Gabriel.Reboul@onera.fr

The first project is taking place in the framework of the Clean Sky Programme [1], a consortium that harnesses the best skills and abilities of over eighty-six organizations representing leading European aircraft manufacturers, research and academic institutes. The global objective of this programme is to minimize the future pollution impact of the aeronautics sector. The project's aim is to test and demonstrate new and innovative technologies that will help to meet the emission and noise reduction targets set by the Advisory Council for Aeronautics Research in Europe (ACARE). Within the subproject GRC7 (Green RotorCraft 7) a novel approach was adopted by the Green Rotorcraft Integrated Technology Demonstrator (ITD) and the Technology Evaluator (TE), that enables the continual assessment of the reduction in environmental impact due to these developing Clean Sky technologies. This approach requires the computation of a large number of flight conditions in order to fill in the database of the consortium noise prediction tool, HELENA [2].

The second project is an ONERA Research Programme, PRF CREATION [3], where a multidisciplinary platform for preliminary studies and new concepts is being designed and developed. In this project, a fast prediction program is needed as a complement of the more precise but more time consuming ONERA comprehensive code HMMAP [4].

In both projects, acoustic predictions are based on the flight mechanics tool EUROPA. EUROPA was originally developed in the framework of a European Project called RESPECT [5] (Rotorcraft Efficient and Safe ProcEdures for Critical Trajectories). The code was specified and developed in order to bring a common tool to the project team, capable of simulating critical flight conditions such as OEI operations (One Engine Inoperative) or Height-Velocity diagram generation flight tests. The physical model is based on Padfield equations of flight dynamics as described in [6]. It is consequently relevant that the new acoustic tool should be at the same level of modelling as EUROPA.

In order to respond to this demand the code *Flap* has been developed. This code is an analytical model aiming to predict the noise emitted by the main rotor of a helicopter with emphasis on the loading noise due to blade-vortex interaction (BVI) known to be dominant in approach configuration. This paper is aiming to present this code.

The methodology employed in *Flap* is similar to the approach adopted in comprehensive code but each step has been simplified. This paper will show how these simplifications affect the results in terms of acoustic radiation and noise sources. The first part of the paper presents a reference computation obtained with HMMAP on the baseline case of the HART II program [7]. Then, the use of a prescribed wake is analyzed. To do it, the free wake code of HMMAP is replaced by a prescribed wake. The third part of the paper deals with the blade loading. An analytical blade response model based on the previous work of Filotas [8] is presented and compared to the singularity method implemented in the code ARHIS of the HMMAP chain. Since the HART II test case is an isolated rotor and the code EUROPA is only developed for a complete helicopter, another test case, based on an AS365N rotorcraft, will be presented in the last part of this paper. The test consists in a comparison of two noise computations performed by *Flap* on the same flight case. The first one is done over a flight condition provided by the EUROCOPTER full flight dynamics code HOST [9], whereas the second one is performed with EUROPA.

1 REFERENCE COMPUTATION

1.1 Presentation of the Onera comprehensive code HMMAP

HMMAP, the computational methodology used at ONERA to predict BVI noise is divided in five main steps: HOST, MESIR, MENTHE, ARHIS, PARIS.

HOST (Helicopter Overall Simulation Tool) is the EUROCOPTER flight dynamics code. The code is jointly shared with ONERA in order to take advantage of ONERA continuous model improvements in different rotorcraft research fields (aerodynamics, acoustics, flight dynamics, loads and vibrations, etc.). The code, mainly dedicated to full flight dynamics simulations, can also address isolated rotor computation. Moreover, the rotor module can perform aeroelastic computations. In the last years, a number of weak

or strong couplings have been realised between HOST and the ONERA comprehensive aerodynamics codes (MINT, MESIR, METAR) or CFD code (*elsA*). In this paper, the code is used to find the rotor trim conditions taking into account aerodynamic, inertial and elastic forces and moments on the blades. The aerodynamic model is based on lifting line method using two-dimensional airfoil tables. In the METAR model [10], the wake model is defined by a prescribed helicoidal geometry described by vortex lattices. A coupling between HOST and METAR is made until convergence so that the rotor trim accounts for vortical wake and blade flexibility.

The prescribed wake geometry is then distorted by using the free wake code MESIR [11].

An intermediate step between wake geometry and blade pressure calculation is introduced using the code MENTHE [12]. During the roll-up process of the vortices, MENTHE identifies the portion of vortex sheets that MESIR calculated as having sufficiently strong intensity to roll-up.

Blade pressure distribution is then calculated by an unsteady singularity method in ARHIS [13]. It performs 2D by slices calculations and the flow is assumed inviscid and incompressible. Consequently, subsonic compressibility as well as finite span effects are included using corrections. The interacting vortices are modeled as freely convecting and deforming clouds (in practice during strong interactions) of vortex elements.

The noise radiation is computed by the code PARIS [14] using the pressure distribution calculated from ARHIS. The PARIS code is based on the Ffowcs Williams-Hawkings equation and predicts the loading and the thickness noise. It uses a time domain formulation with an efficient spanwise interpolation method, which identifies the BVI impulsive events on the signatures generated by each blade section.

1.2 Test case definition

The test case used in the first part of this paper is the baseline case of the HART II test campaign. The second High harmonic control Aeroacoustic Rotor Test (HART II) [7] was conducted in 2001 by a joint multi-national effort of the DLR (Germany), AFDD and NASA Langley (USA), ONERA (France) and DNW (Netherlands). Numerous measurements including section airloads, tip vortex positions and acoustic radiation were performed in the 8m $\times$ 6m cross-section of the DNW wind tunnel in open-jet configuration. The model is a 40% Mach scaled Bo105 rotor. The reference operating condition for the baseline case as well as the rotor geometry are defined in table 1.

Rotor radius, R	2 m
Blade chord, c	0.121 m
Root radius	0.44 m
Number of blades, B	4
Airfoil	NACA23012
Twist	-8°/R
Radius of zero twist	1.5 m
Wind speed, V_0	32.9 m/s
Speed of sound, c_0	341.7 m/s
Rotational speed, Ω	109 rad/s
Thrust, T	3300 N
Rotor shaft angle of attack, α_s	5.3° (4.5° with wind tunnel interference)

Table 1: Baseline test case of the HART II program

1.3 Reference results

The following figures present a comparison between experimental data and results obtained using HMMAP. Figure 1 exposes the sectional load at 87% of span.

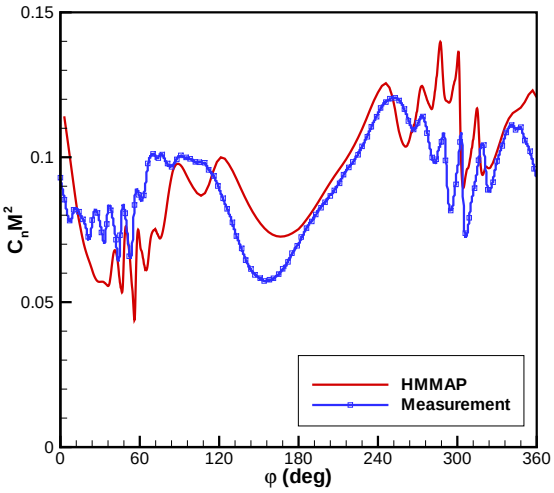

Figure 1: Normal force coefficient at $0.87R$

Good correlations are obtained in terms of amplitude of the low frequencies (due to blade

motion) and high frequencies (due to BVI). Some shifts are visible on the advancing side and for the minimum value ($\varphi = 154°$ for the measurement and $\varphi = 168°$ for HMMAP). Also some small interactions are missing at the beginning of the advancing side.

Figures 2 and 3 are noise carpets in dB. Frequencies lower than the 6th blade passage frequency (BPF) and higher than the 40th are filtered to highlight the acoustic radiation due to BVI. The wind direction is denoted by the black arrow and the rotor disk by the black circle.

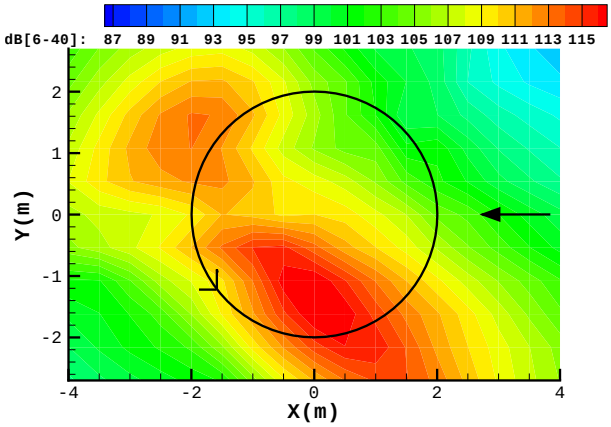

Figure 2: Noise footprint in dB [6-40 BPF]: HMMAP

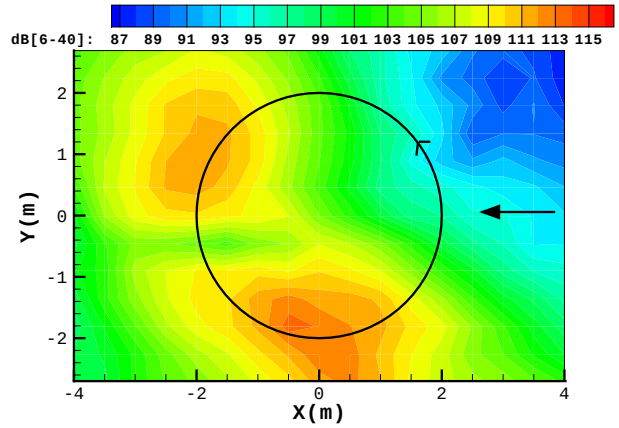

Figure 3: Noise footprint in dB [6-40 BPF]: Measurement

One can notice a good agreement of the directivities on the advancing side but the noise levels are over-predicted by 3.5 dB. Concerning the retreating side, the directivity is still good and the predicted noise levels are closer to the experiment compared to the advancing side predictions (1.48 dB).

2 PRESCRIBED AND FREE WAKE COMPARISON

The aerodynamic part of the chain is certainly the most important since it determined the blade-vortex distance, known to have a major impact on BVI noise. On the other hand, this part is also the most time consuming when a free wake code is considered. One way to reduce significantly the computational time is to use a prescribed wake. Several downwash models [15, 16] exist and can provide the induced velocity distribution across the rotor disk. The model of Beddoes [17] is one of these models and has the advantage to provide the induced velocity and consequently the vortex position inside and outside the rotor disk which is necessary when using ARHIS and *Flap*. This model has already been used for BVI noise prediction. In [18], the Beddoes model is used as an input in an Euler solver. This model is also used with some improvements in the DLR comprehensive code S4 [19, 20]. The next part of the paper briefly described how this model is used in *Flap* and what is the impact of using it by comparison with a free wake code.

2.1 Wake geometry

The model used in *Flap* is very close to what was originally proposed by Beddoes. One assumption made in *Flap* is that only interactions between tip vortices and blades are considered. Even if this kind of interaction is dominant, other vortices can be created inside the rotor disc and be responsible of noisy interactions. The blade flapping is taken into account in the vertical displacement of the vortices. To respect the momentum theory, the corrections proposed by van der Wall in [19] are implemented as in [18].

Figure 4 is a 3D view of the tip vortex convection provided by both free wake code (MESIR) after roll up (by the code MENTHE) and the semi-empirical model of Beddoes.

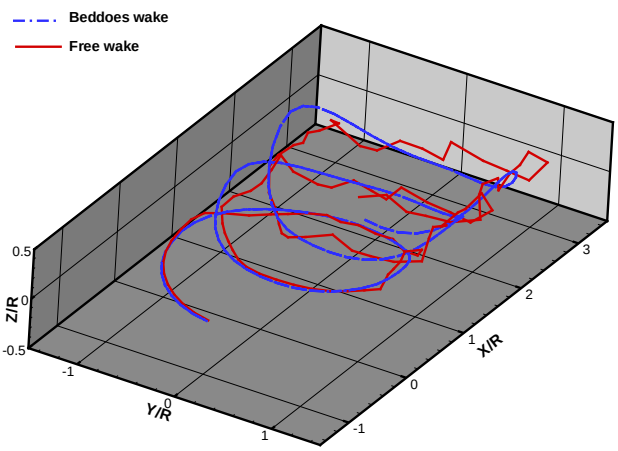

Figure 4: Comparaison of the tip vortex position provided by the free wake code MESIR and by the semi-empirical model of Beddoes: 3D view

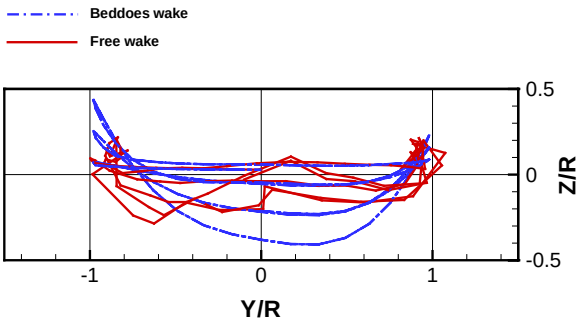

Figure 5: Comparaison of the tip vortex position provided by the free wake code MESIR and by the semi-empirical model of Beddoes: Front view

The general behavior of the wake convection is clearly assessed by the Beddoes model. A front view of the same comparison is presented in figure 5. On the retreating side (right part), the two wakes have similar height. In the middle part, the free wake code goes higher than the prescribed wake. The model over-estimates the downwash in this part of the disc since the lifting part of the blade is assumed to extend to the rotor center. On the contrary, on the advancing side, the Beddoes model predicts a higher wake. This last point will have a strong impact on the noise radiation, this is why further analysis are proposed here after.

Figure 6 displays the tip trajectories in advancing side at y=0.7R. A good agreement is observed in the front part even if the two prediction methods are below the experimental measurement. For $x > 0$, the prescribed wake stays very high and does not have the same slope than the measurement and the free wake code. This will certainly cause earlier interactions.

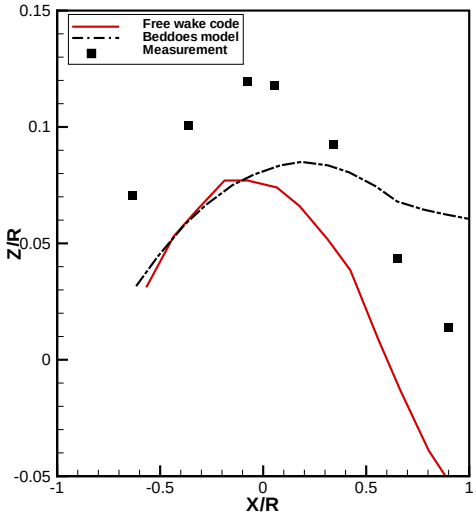

Figure 6: Tip trajectories on the advancing side at y=0.7R

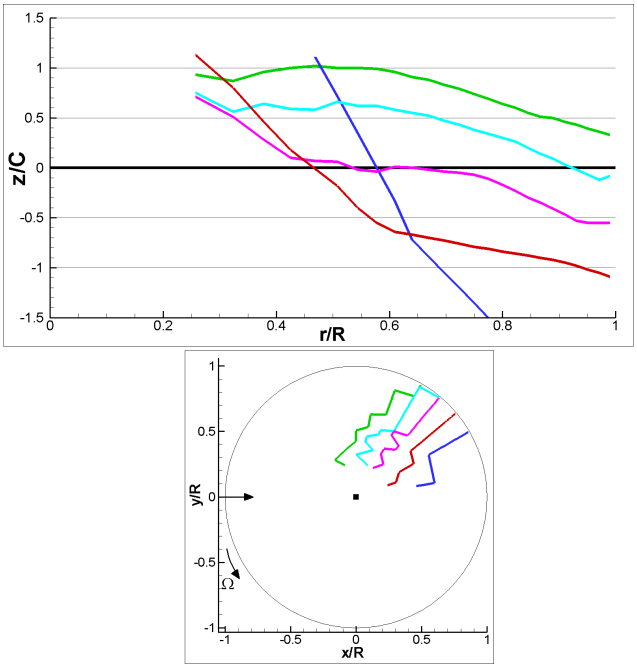

Figure 7: Interactions analysis when using the free wake code

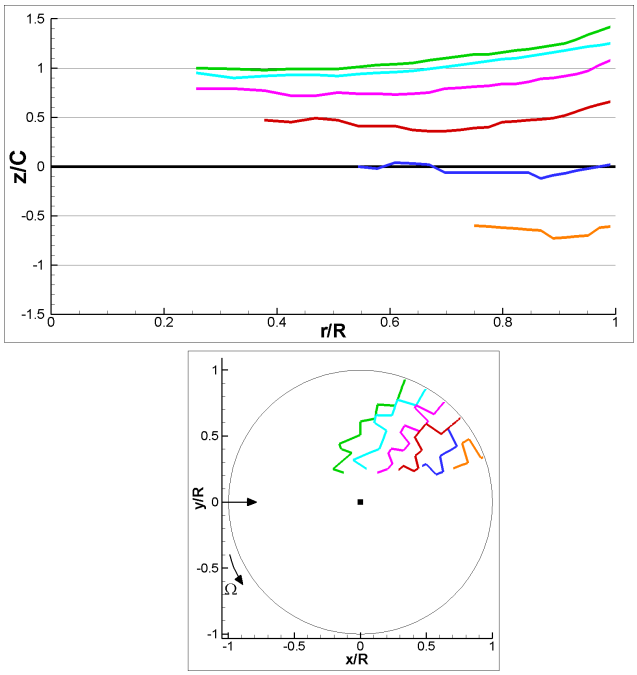

Figure 8: Interactions analysis when using the Beddoes model

This analysis is confirmed by figures 7 and 8, allowing to visualized the blade-vortex distance on the top part and the azimuth of the corresponding interactions on the bottom part of the figure. With the prescribed wake, almost all the vortices go up to the blade and a very strong interaction occurs (blue line) at a low azimuth. With the free wake code, part of the vortices goes above and the other ones below the blade. The two mains interactions are produced by the cyan and the pink vortex line at a higher azimuth angle. The more early are the interactions, the more the vertical angle between the vortex line and the blade increases, while with the prescribed wake the interactions stay parallel increasing by this fact the interaction efficiency.

2.2 Vortex intensity

Since the geometry of the wake is determined, it is now necessary to compute the strength of the vortices. The vortex strenght is closely related to the blade circulation and consequently to the blade loading. The blade loading is computed using a classical blade element analysis with linear aerodynamics. The lift coefficient on a blade element is given by equation 1.

(1) $$Cl = Cl_\alpha \alpha$$

Cl_α is the lift curve slop and α is the aerodynamic angle of attack decomposed as in equation 2. θ is pitch angle, θ_v is the angle induced by the blade twist, α_0 is the zero-lift angle of attack of the blade section and U_p and U_t are respectively the normal and tangential velocities.

(2) $$\alpha = \theta + \theta_v - \alpha_0 - tan^{-1}\left(U_p/U_t\right)$$

Computations of local velocities , U_t and U_p, are then necessary and performed by solving equations 3 and 4. In equation 4, the induced velocity field, ν, is obtained from the Beddoes model.

(3) $$U_t = \Omega r + V_0 cos(\alpha_s) sin(\varphi)$$

(4) $$\begin{aligned} U_p &= -V_0 sin(\alpha_s) + \nu + r\dot{\beta} \\ &+ c/4\dot{\theta} + V_0 cos(\alpha_s)\beta cos(\varphi) \end{aligned}$$

Cl_α, θ_v and α_0 are direct input data of the code. θ and β are provided by the flight mechanics code, in this case HOST. Here, Cl_α and α_0 are adjusted to match the behavior of the code ARHIS for low angle of attack.

Some additional corrections are implemented. Like in ARHIS, subsonic compressibility effects are included by means of Prandtl-Glauert corrections (in ARHIS, this correction is combined with a local thickening of the airfoil). In addition, finite span effects are introduced through an elliptic-type correction of lift coefficient.

Since only the tip vortex is considered, the whole vortex sheet is supposed to roll up into the tip vortex. Consequently, the vortex strength, Γ is supposed to be equal to the maximum of blade circulation along the span at each emission time. However, the predictions have provided values of circulation too high compared to HMMAP results. One hypothesis is that the vortex circulation is not equal to the maximum of blade circulation along the span and some part of the circulation is dissipated in the inboard vortex sheet as well as in the creation of counter rotating vortices. In [21],

Komerath et al. find a ratio of 0.4 between the tip vortex circulation and the maximum blade circulation for an untwisted blade. For a twisted blade with an aspect ratio of 10, McAlister [22] founds a ratio of 0.7. In our case, with a higher aspect ratio (16.5), a value of 0.85 has been applied.

Finally, the vortex intensity as a function of age for the two wakes is presented in figure 9.

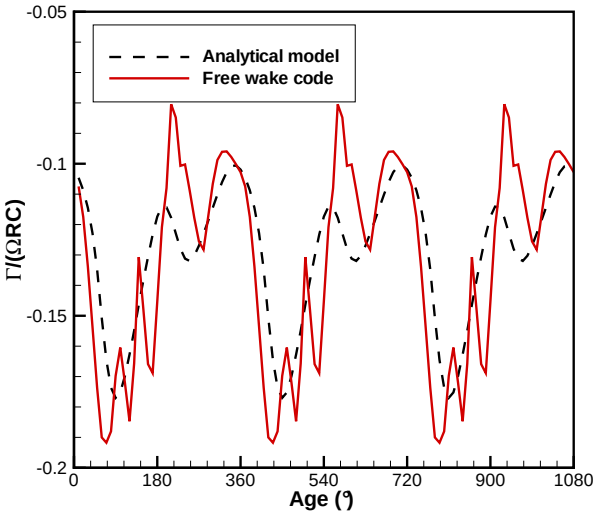

Figure 9: Vortex intensity as a function of age

The mean part as well as the low frequencies variations are in good agreement but the free wake code provides some extra variations.

2.3 Acoustic results

To assess the impact of using the prescribed wake, the vortex intensity model as well as the induced velocity distribution and the wake geometry provided by the model of Beddoes are used as an input in the ARHIS code instead of the data obtain by MESIR and MENTHE.

The previous observations concerning the wake (cf. 2.1) are directly visible when having a look at the normal force coefficient (figure 10) and the noise footprint (figure 11).

Since the same blade kinematics are used in each computations, the low frequencies discrepancies are due to the induced velocity distribution. Concerning the BVI, the strong and early interaction already noticed in 2.1 is clearly visible. On the contrary, retreating side interactions are well in phase.

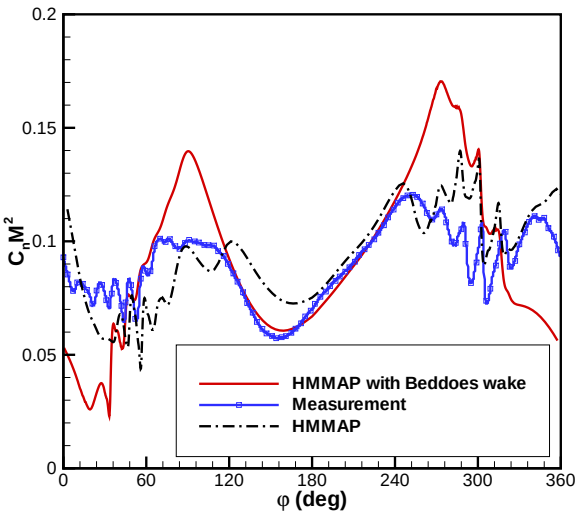

Figure 10: Normal force coefficient at $0.87R$

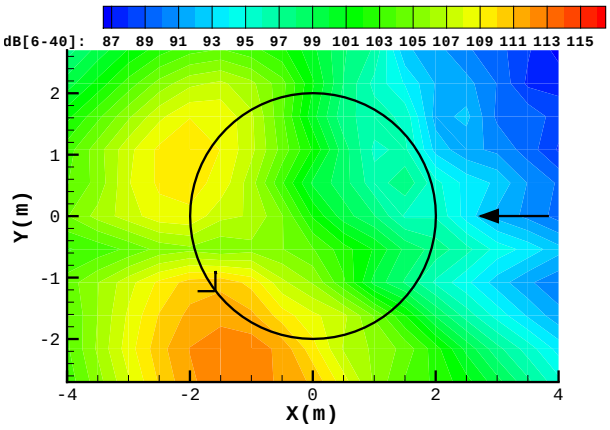

Figure 11: Noise footprint in dB [6-40 BPF]

Consequently, the directivity on the retreating side is in good agreement with the experiment and the acoustic levels are slightly underestimated (-1.88 dB). On the advancing side, even if the main interaction seems very impulsive, the azimuth of interaction is too low to create an important noise radiation. Hence, levels are also under-estimated (-0.87 dB) and the directivity is, as expected, shifted downwind.

One way of improvement comes from an empirical modification of the coefficient used in the Beddoes model to increase the downwash on the advancing side. The radial position of the tip vortex can also be adjust (generally a bit inboard). Other improvements that need to be investigate are proposed by van der Wall [19] by reducing the lifting part of the blade contributing to the downwash.

3 ANALYTICAL BLADE RESPONSE FUNCTION

The use of a prescribed wake allows to greatly reduce the computational time. CPU time decreases from approximately 1 hour to 2 minutes. However, a blade surface discretization is still necessary. Since it is not the case in EUROPA, further simplifications of the computational chain are still needed. Thus, it is possible to determine the blade pressure with an analytical blade response with a compact chord approach. The next section deals with the presentation of this model and the results obtained while using it.

3.1 The compact chord approach

In this section, the blade pressure is still computed with the code ARHIS but the pressure is integrated to obtain a solution compact in chord. Then, the code PARIS in a compact chord formulation is used to obtain the acoustic radiation.

The impact of using a compact chord approach can be estimated by looking at the noise footprint obtained with this method in figure 12 and make the comparison with figure 11.

Very small differences are observed. As expected, the noise spectra at the maximum noise location presented in figure 13 show almost no differences in low frequencies. Discrepancies become noticeable after $2kHz$, i-e above the BVI frequency range.

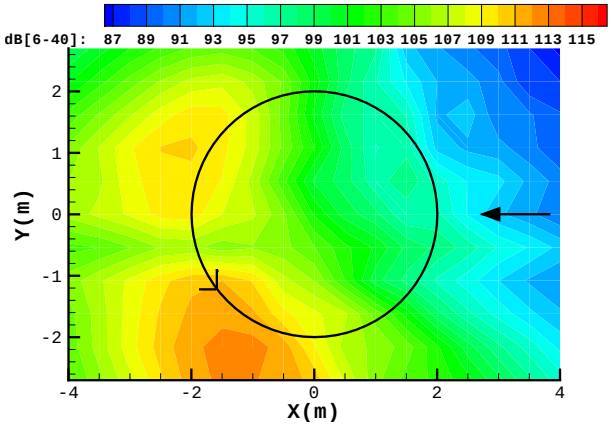

Figure 12: Noise footprint in dB [6-40 BPF] using a compact chord approach

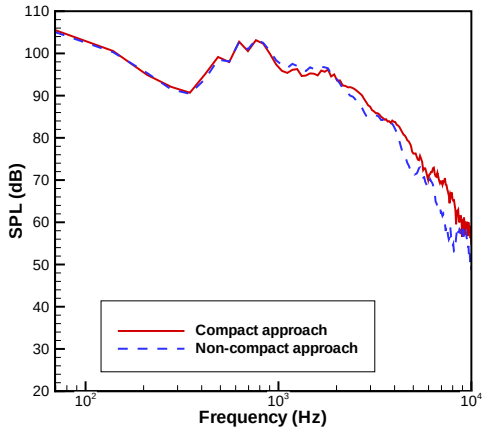

Figure 13: Noise spectra at the maximum noise location

Concerning the thickness noise, the blade profile is necessary. This noise contribution is clearly insignificant compared to BVI and can often be neglected. However, if the acoustic radiation due to the thickness noise is desired, it is possible to restrict the number of input data to the chord and the maximum thickness of the airfoil. Then, the blade profile can be obtained from classical parametrized airfoil shape like the NACA00XX (XX being the relative maximum thickness) airfoil. Since helicopter airfoils have generally small camber, the errors induced by this method is very small. The two possibilities (to reconstruct an airfoil geometry or to neglect thickness noise) are available in *Flap*.

3.2 Blade loading

Two main orientations are possible, the time or the frequency domain approaches. The time domain solution is based on the indicial response method presented in [23] and used in [20]. This method requires the resolution of Duhamel integral but has the advantage, contrary to the frequency domain approach, not to be restricted to steady problems. However, the prescribed wake model used in the previous part is also limited to periodic blade motion. This is why, a frequency domain approach has been chosen in this study.

The goal is only to determine the blade pressure fluctuation resulting from the BVI. The low frequency content is obtained from BEMT approach presented in section 2.2. In order to link the incident velocity fluctuations (i-e the vortex)

to the unsteady surface pressure on the blade, Sears [24, 25] proposed a model based on the linear theory of thin airfoil. Sears studies were reexamined by Filotas [26], and adapted for BVI by Widnall [27] and Filotas [8]. The approach of Filotas is retained in this study. The problem of BVI (illustrated in figure 14) is simplified by considering an airfoil (assimilated to a flat plate) convected uniformly at the velocity $U_c = \Omega r$ with an angle χ and a distance h from an infinity of vortices of circulation Γ.

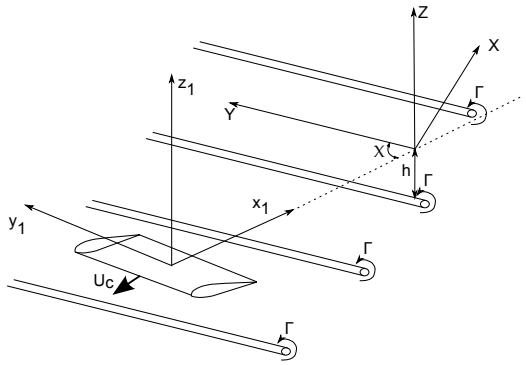

Figure 14: Simplified representation of a blade vortex interaction

By doing this simplification, the model fails to account for rotation , which would introduce a linear spanwise velocity gradient of the free stream. This velocity gradient be can neglected by comparison with vortex induced velocity.

The spanwise discretization of the blade is identical to what is used in HMMAP (26 sections) and the number of azimuthal steps is increased linearly from the root to the tip of the blade ($1.3°$ to $0.3°$). Like in ARHIS, interactions are selected depending on the vortex characteristics (χ, Γ and h). These parameters are averaged with a weight based on the distance between the segments of vortex considered and the blade.

Following [8], the strength per span unit is given by :

$$dF = \pi\rho U_c c W(k) Sg(bk,\chi) e^{iksin(\chi)U_c t} \quad (5)$$

where b is the semi-chord, k is the aerodynamic wave-number ($k = \omega/U_c$), $W(k)$ is the spatial Fourier transform of the upwash velocity fluctuations and Sg is the aerodynamic transfer function. This function writes:

$$Sg(bk,\chi) = \frac{2}{\pi kb\left[H_0^{(1)}(bk) + iH_1^{(1)}(bk)\right]} \times \frac{2J_1(bkcos\chi)}{bkcos\chi} \quad (6)$$

where $H_0^{(1)}$ and $H_1^{(1)}$ are respectively the Hankel functions of first species and of order 0 and 1. J_1 is the Bessel function of first order. Now, the incident velocity perturbations need to be defined. The vertical velocity of a point vortex is equal to:

$$w_t = \frac{\Gamma}{2\pi}\frac{X}{X^2+h^2} \quad (7)$$

The spatial Fourier transform of w_t is given by equation 8 :

$$W_t(k) = \frac{i\Gamma}{4\pi}\frac{k}{|k|}e^{-|k|h} \quad (8)$$

The influence of the fluctuating streamwise component of the vortex induced velocity is neglected since the resulting loads is an order smaller than the loads due to upwash component (cf. [8]). If an infinity of vortices equally spaced by a distance $d = 2\pi Rsin\chi$ is considered, the wave-number spectrum becomes:

$$W(k) = \frac{2\pi}{d}W_t(k)\sum_{n=-\infty}^{+\infty}\delta\left(k+\frac{2\pi n}{d}\right) \quad (9)$$

h may be considered as an effective height that account for the viscous core radius of the vortex, denoted by r_c. Once again as in ARHIS, a semi-empirical law proposed in [28] is used to determined the viscous core radius. From test computations with ARHIS using different value of r_c and h, it is possible to observe a limitation of the blade response when $h < r_c/2$. Consequently, a limitation is implemented so that h cannot be smaller that $r_c/2$.

The dissymmetry between advancing and retreating side interactions is taken into account through the use of a relative velocity ($U_c = \Omega r + V_0 cos(\alpha_s) sin\varphi$) instead of the rotational velocity in equation 5.

Finally, the acoustic radiation code being formulated in the time domain, the previous result is

inverse Fourier transformed and the total blade loading resulting from multiple BVI is obtained by superposition of the model problem result.

Figure 15 is a view of the normal force coefficient obtained with *Flap* and ARHIS.

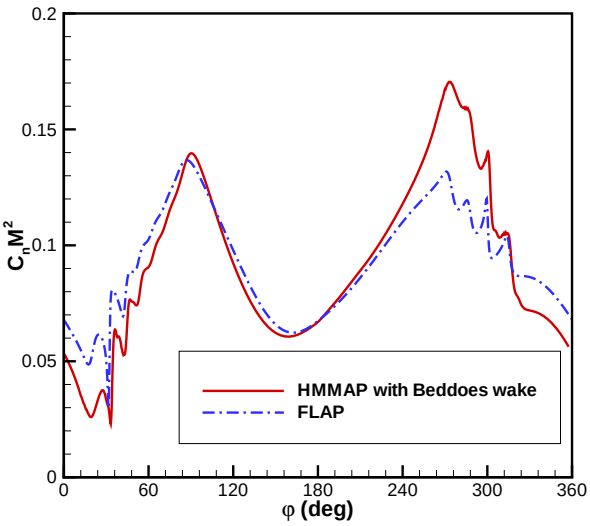

Figure 15: Normal force coefficient at $0.87R$

Two main discrepancies can be observed. First, the main interaction on the advancing side is over-estimated. One can conclude that the model over-estimates the blade response to strong interactions even with a limitation on the blade-vortex distance. This is certainly due to viscous core effect and vortex deformation that occur during such events. The second major discrepancy concerns the low frequency content during azimuthal range of BVI. This could be linked to the effect of BVI on the mean loading of the blade. However, this won't have a strong effect on the noise radiation which is dominated by the BVI noise. Except for these points, the two results are in relatively good agreement. Concerning, the rotor thrust, ARHIS gives $3165N$ while *Flap* obtain $3216N$ which is even closer to the experimental value of $3300N$.

3.3 Acoustic radiation

The acoustic radiation provided by the code *Flap* is presented in Figure 16.

Very little differences are observed between figure 16 and 12. The directivities are almost the same. But the advancing side noise level is a increased by 0.7 dB at the maximum. On the other hand, the noise levels on the retreating side is a bit decreased. In this computation, the thickness noise is obtained with a NACA0012.

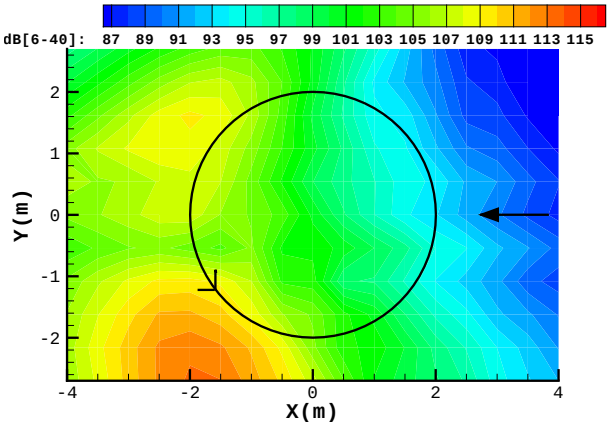

Figure 16: Noise footprint in dB [6-40 BPF] provided by the *Flap* code

A last analysis of the results provided by *Flap* can be made by observing the 1/3 Octave spectra in figures 17.

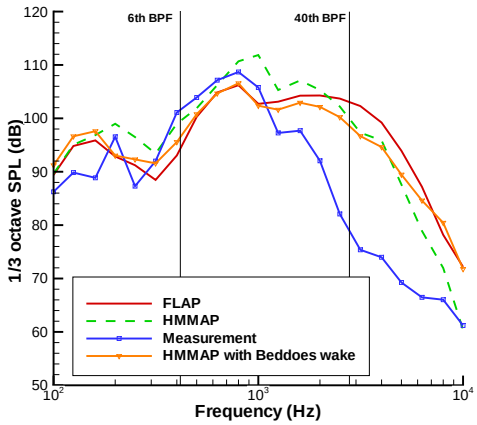

Figure 17: 1/3 octave noise spectra at the maximum noise location

As expected, the spectra obtain by *Flap* and ARHIS with the same wake geometry and intensity are in good agreement. This is true except for high frequencies probably because of the higher impulsivity of the main interaction. On can remark that all the method predict higher noise level in high frequencies. The bump characteristic of BVI noise between 500 Hz and 1200 Hz approximately is well assessed by all the methods. It proves that the physics of the phenomena is well captured.

To conclude, the code *Flap* allows to predict with a relatively good precision the noise level on 200 observers in 20 seconds with a limited number of input data. Some improvements are still possible and concern the wake geometry which seems to be the weak link of the computational chain.

4 EUROPA INSTEAD OF HOST

In the previous sections, the blade kinematics has been provided by the code HOST. Since *Flap* is devoted to be coupled to EUROPA, the last part of the paper deals with an analysis of the effect of flight dynamics computations quality on noise prediction. Therefore, a comparison between EUROPA and HOST is presented hereafter.

EUROPA is not developed for isolated rotor computations. Therefore, simulations are performed on a complete helicopter. The selected test case is the AS365N Dauphin helicopter on a 6° descent flight at 70 kts.

4.1 Thrust and blade kinematics comparison

Table 2 shows the values used as input in *Flap* provided by both flight mechanics code.

	EUROPA	HOST
Thrust	33955 N	31547 N
θ_0	2.21°	1.863°
θ_1^c	0.966°	1.310°
θ_1^s	-0.737°	-0.693°
β_0	2.244°	1.661°
β_1^c	-1.219°	-1.515°
β_1^s	-0.430°	-0.536°
α_s	2.42°	2.59°

Table 2: Comparison of EUROPA and HOST concerning the blade kinematics, thrust and rotor angle of attack

These values are the thrust, the blade kinematics and the rotor angle of attack. Concerning, the blade kinematics, the harmonic decomposition is here limited to the first harmonic since EUROPA cannot provide higher value. The subscript 0 denotes the mean value and the superscript c and s represent respectively the cosine and the sine terms. However, in section 1 to 3, the decomposition has been made up to the fifth harmonic rank. The main difference concerns the thrust. EUROPA provides a higher thrust with a discrepancy of 2408 N. Concerning the blade kinematics, the angles obtained by both codes are in good agreement, the higher difference being of 0.58° on the coning angle.

4.2 Effect on acoustic radiation

Like in EUROPA, the chord and the airfoil profile defined in *Flap* are supposed to be constant in the spanwise direction. Consequently, mean values have to be defined. Table 3 summarizes the geometrical characteristics of the rotor used.

R	5.965 m
c	0.405 m
Flapping hinge offset	0.23 m
Root radius	1.69 m
B	4
Twist	-1.71°/R
Radius of zero twist	0.95R
Cl_α	5.79 rad
α_0	-1.5°
Ω	350 RPM
Rotor shaft angle	-4°

Table 3: Geometrical characteristics of AS365N main rotor

Since the flight mechanics codes and *Flap* do not use the same induced velocity model and load prediction method, it could be hard to obtain the same rotor thrust, which is, as shown here after, a key parameter. Hence, if the thrusts (input and calculated) differ by more than 1%, then an iterative process is engaged by increasing or decreasing the collective pitch angle until convergence. In both cases, the collective pitch angle is only increased by $0.2°$.

Figure 18 and 19 are illustrations of the noise footprint 150 m below the rotorcraft (represented by the black circle). The reference frame is identical to a wind tunnel frame with an horizontal wind speed and a rotor tilted upward (for an approach configuration). The wind direction is denoted by the black arrow.

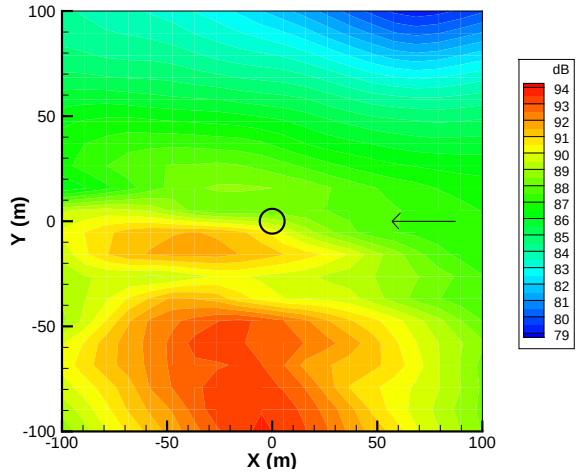

Figure 18: Noise footprint in dB provided by the EUROPA-*Flap* codes

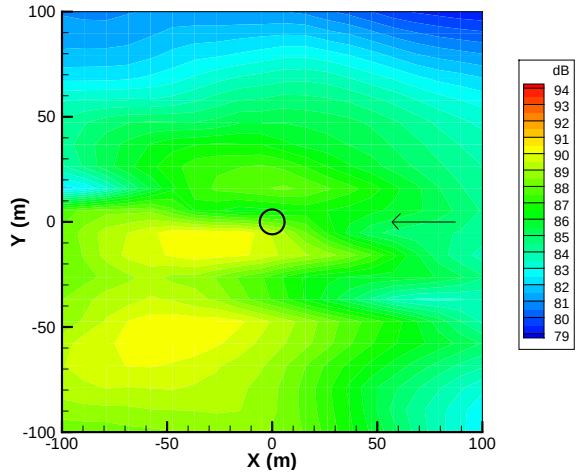

Figure 19: Noise footprint in dB provided by the HOST-*Flap* codes

The directivities obtained are relatively close but discrepancies are noticeable in terms of noise level. The prediction provided by the chain EUROPA-*Flap* is 3.2 dB higher at the maximum. This is clearly due to the different rotor thrust. First, a higher thrust induces higher vortex circulation and consequently higher noise level. Secondly, as one can see on figure 20 and 21 showing blade-vortex distances and angles analysis on the advancing side, the wake is more convected downward with an increase of thrust. This causes main interactions to occur later during the rotation and increases the efficiency in an acoustic point of view. Moreover, this interaction (denoted by the red line) arises on a larger part of the blade span.

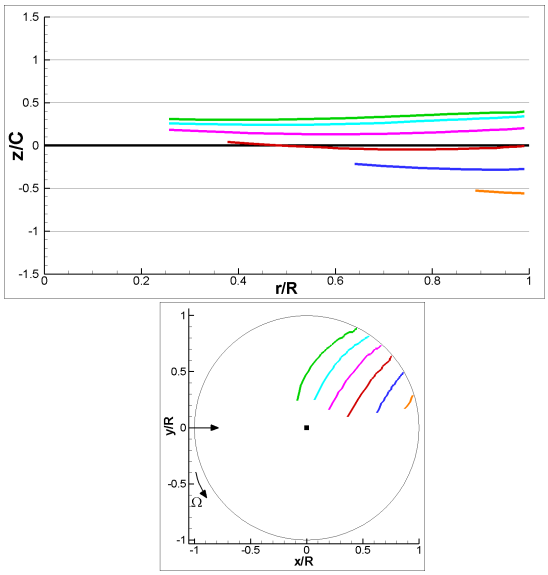

Figure 20: Interactions analysis when using the EUROPA-*Flap* codes

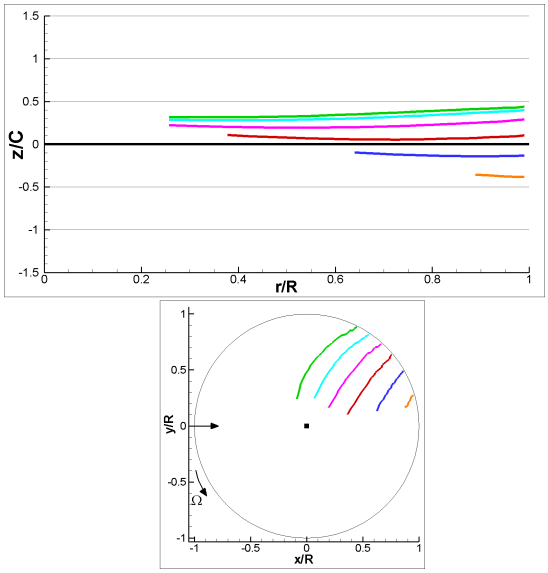

Figure 21: Interactions analysis when using the HOST-*Flap* codes

From this analysis, it is clear that the total thrust is a key parameter in the prediction of main rotor noise in a flight dynamics perspective. Even if EUROPA is able to provide good predictions of the blade kinematics (by comparison with HOST), the difference in thrust induced discrepancies in terms of acoustic radiation.

However, it should be noted that these discrepancies are commonly noticed in such comparisons between flight dynamics tools. Different techniques can be used in order to reduce

these discrepancies through a calibration of the models. Particularly in this test case, the quality of the HOST code simulation is much higher since the code is largely calibrated with EUROCOPTER flight data. The same process can be applied to EUROPA in order to better capture the real Dauphin flight data and consequently the noise level.

CONCLUSION

An analytical model, named *Flap*, has been developed in order to obtain fast predictions of main rotor helicopter noise, taking into account the blade-vortex interactions by using input data from the flight mechanics code EUROPA. Comparisons with measurements and the Onera comprehensive acoustic code HMMAP are satisfying. It proves that the physics of the phenomena are well captured and that the code can be used for preliminary studies at least for relative comparisons. This is especially true if one considers the complexity of the phenomena, the relative simplicity as well as the speed of the model (approximately 20 seconds for 200 microphones).

The wake prediction used in *Flap* is based on the Beddoes prescribed wake model. By using this model in HMMAP instead of a free wake code, one can clearly see that this part is the weak link in the chain if the flight mechanics is hold apart. Thus, some possibilities of improvement are proposed. On the contrary, the use of a compact chord approach with an analytical modelling of the blade pressure does not impact too much (except for very close interactions) the acoustic radiation compare to a singularity method.

In the last part of the paper, comparisons between the numerical code HOST and analytical code EUROPA show that total thrust prediction can also greatly impact the noise radiation since it changes the blade-vortex distances and vortex strengthes.

Since *Flap* provides relatively good and very fast prediction, together with some improvements, it is now planned to use this code for low noise flight procedures. The main difficulty will be to deal with the stationary nature of the code.

ACKNOWLEDGEMENT

This project is partly funded by the European Union in the framework of the Clean Sky program - Green Rotorcraft. This financial support is gratefully acknowledged.

References

[1] A. Antifora and F. Toulmay. CLEAN SKY - The GREEN ROTORCRAFT integrated technology demonstrator-state of play three years after kick-off. In *Proceedings of the 37th European Rotorcraft Forum, Ticino Park, Italy*, 2011.

[2] M. Gervais, V. Gareton, A. Dummel, and R. Heger. Validation of EC130 and EC135 environmental impact assessment using HELENA. In *Proceedings of the 66th AHS Annual Forum, Phoenix, USA*, 2010.

[3] P.-M. Basset, A. Tremolet, F. Cuzieux, C. Schulte, D. Tristrant, T. Lefebvre, G. Reboul, M. Costes, F. Richez, S. Burguburu, D. Petot, and B. Paluch. The C.R.E.A.T.I.O.N. project for rotorcraft concepts evaluation: The first steps. In *Proceedings of the 37th European Rotorcraft Forum, Ticino Park, Italy*, 2011.

[4] P. Beaumier and Y. Delrieux. Description and validation of the onera computational method for the prediction of blade-vortex interaction noise. In *Proceedings of the 29th Europeen Rotorcraft Forum*, 2003.

[5] C. Serr, G. Polz, J. Hamm, J. Hughes, M. Simoni, A. Ragazzi, A. Desopper, A. Taghizad, H.J. Langer, C. Young, A. Russo, A. Vozella, and J. Stevens. Rotorcraft efficient and safe procedures for critical trajectories. *Air and Space Europe*, 3 (3/4):266–270, 2001.

[6] Gareth D. Padfield. *Helicopter Fligh Dynamics*. Blackwell Publishing, 2007.

[7] B.G. van der Wall, C.L. Burley, Y.H. Yu, K. Pengel, and P. Beaumier. The HART II test - measurement of helicopter rotor wakes. *Aerospace Science and Technology*, 8 (4), 2004.

[8] L.T. Filotas. Vortex induced helicopter blade loads and noise. *Journal of Sound and Vibration*, 27(3):387–398, 1973.

[9] B. Benoit, A.-M. Dequin, K. Kampa, W. Grunhagen, P.-M. Basset, and B. Gimonet. HOST: A general helicopter simulation tool for germany and france. In *Proceedings of the 56th AHS Annual Forum, Virginia Beach, USA*, 2000.

[10] G. Arnaud and P. Beaumier. Validation of R85/METAR on the Puma RAE flight tests. In *Proceedings of the 18th European Rotorcraft Forum, Avignon, France*, 1992.

[11] B. Michea, A. Desopper, and M. Costes. Aerodynamic rotor loads prediction method with free wake for low speed descent. In *Proceedings of the 18 European Rotorcraft Forum, Avignon, France*, 1992.

[12] G. Rahier and Y. Delrieux. Blade-vortex interaction noise prediction using a rotor wake roll-up model. *Journal of Aircraft*, 34 (4):522–530, 1997.

[13] G. Rahier and Y. Delrieux. Influence of the vortex models on blade-vortex interaction load and noise predictions. *Journal of the American Helicopter Society*, 44(1):26–33, 1994.

[14] P. Spiegel and G. Rahier. Theoretical study and prediction of BVI noise including close interactions. In *Proceedings of the AHS Technical Specialists Meeting on Rotorcraft Acoustics and Fluid Dynamics, Philadelphia, USA*, 1991.

[15] J.M. Drees. A theory of airflow through rotors and its application to some helicopter problem. *J. Helicopter Assoc. Great Britain*, 3(2), 1949.

[16] K.W. Mangler and H.B. Squire. The induced velocity field of a rotor. Technical report, ARC R&M 2642, 1950.

[17] T. S. Beddoes. A wake model for high resolution airloads. In *Proceedings of the 2nd International Conference on Basic Rotorcraft Research, Triangle Park, USA*, 1985.

[18] Y. Inada, C. Yang, N. Iwanaga, and T. Aoyama. Efficient prediction of BVI noise using Euler solver with wake model. In *Proceedings of International Forum on Rotorcraft Multidisciplinary Technology, Seoul, Korea*, 2007.

[19] B.G. van der Wall. The effect of HHC on the vortex convection in the wake of a helicopter rotor. *Aerospace Science and Technology*, 4:321–336, 2000.

[20] B.G. van der Wall. Simulation of active rotor control by comprehensive rotor code with prescribed wake using HART II data. In *Proceedings of the 65th AHS Annual forum, Grapevine, USA*, May 2009.

[21] N. Komerath, O. Wong, and B. Ganesh. On the formation and decay of rotor blade tip vortices. In *Proceeding of the Fluid Mechanics Meeting*, 2004.

[22] K.W. McAlister. Rotor wake development during the first revolution. In *Proceedings of the 59th AHS annual forum, Phoenix, USA*, 2003.

[23] J.G. Leishman. *Principles of Helicopter Aerodynamics*. Cambridge Aerospace Series, 2000.

[24] T.H. Von Karman and W.R. Sears. Airfoil theory for non-uniform motion. *Journal of the Aeronautic science*, 5(10):379–390, 1938.

[25] W.R. Sears. Some aspects of non-stationary airfoil theory and its practical applications. *Journal of Aeronautical Science*, 8:104–108, 1941.

[26] L.T. Filotas. Approximate transfer function for large aspect ratio wings in turbulent flow. *Journal of Aircraft*, 8(6):395–400, 1971.

[27] S. Widnall. Helicopter noise due to blade-vortex interaction. *Journal of the Acoustical Society of America*, 50:354–365, 1971.

[28] G. Perez, J. Bailly, and G. Rahier. Derivation of new physical models for BVI noise prediction. *Journal of the American Helicopter Society*, 53(1):56–67, 2008.